Defense Technical Information Center Compilation Part Notice

ADP012226

TITLE: Nickel Nanocomposite Thin Films

DISTRIBUTION: Approved for public release, distribution unlimited

This paper is part of the following report:

TITLE: Nanophase and Nanocomposite Materials IV held in Boston, Massachusetts on November 26-29, 2001

To order the complete compilation report, use: ADA401575

The following component part numbers comprise the compilation report:
ADP012174 thru ADP012259

Mat. Res. Soc. Symp. Proc. Vol. 703 © 2002 Materials Research Society V9.12

NICKEL NANOCOMPOSITE THIN FILMS

Honghui Zhou, A. Kvit, D. Kumar, and J. Narayan
Department of Materials Science and Engineering and NSF Center for Advanced Materials and Smart Structures.
North Carolina State University, Raleigh, NC 27695-7916, U.S.A.

ABSTRACT

Nickel was deposited on epitaxial TiN matrix layer grown on Si (100) substrate by pulsed laser deposition process (PLD). Transmission electron microscopy (TEM) study shows that nanoparticles formed are single crystals with two kinds of epitaxial relationship with respect to matrix TiN. One is cube on cube, where (200) Ni // (200) TiN // (200) Si and (02 $\bar{2}$) Ni // (02 $\bar{2}$) TiN // (02 $\bar{2}$) Si. The particles grown in this orientation have a trapezoidal morphology in [011] projection. The other involves a 90 ° rotation with respect to [011] direction of TiN matrix (zone axis), where (0 $\bar{2}$2) Ni // (200) TiN // (200) Si and (200) Ni // (02 $\bar{2}$) TiN // (02 $\bar{2}$) Si. The particles grown in this rotated orientation have a triangular morphology in [011] projection and a smaller lattice constant compared with that of pure nickel. The possible mechanism of forming these two epitaxial orientations is discussed. Superconducting quantum interference device (SQUID) magnetometer was used for magnetic measurements. In order to investigate the effect of texturing on magnetic properties of nanoparticles, results were compared with those obtained from Ni nanoparticles grown on amorphous Al_2O_3 matrix layer in previous research. It was found that both blocking temperature and coercivity of Ni nanoparticles grown on epitaxial TiN matrix are significantly higher than that of Ni grown on amorphous Al_2O_3. The higher value of coercivity is possibly associated with the stronger tendency of crystallographically oriented particles to retain their magnetic moments in the presence of reversing magnetic field.

INTRODUCTION

Nanomagnetic materials have drawn significant attention in recent years due to their dramatically improved physical properties critical for enhancing the magnetic device performance, such as giant magnetoresistance, superparamagnetism, large coercivities, high Curie temperature, and low saturation magnetization [1-7]. Magnetic properties of the nanomagnetic materials are closely related to the magnetic anisotropy of the material, which depends not only on the size, shape and strain state of the particles, but also on their crystal structure and orientation. However, so far, most studies in this area have been focused on the dependence of magnetic properties on the particle size and separation. It is expected that further improvement in these properties could be realized by texturing the magnetic particles along their easy axis. In the present study, epitaxial Ni nanoparticles were grown on TiN thin-film matrix by pulsed laser deposition (PLD) technique. The crystalline quality of the particles was investigated by conventional and high-resolution transmission electron microscopy (TEM and HRTEM). In order to investigate the effect of texturing of magnetic particles on their magnetic properties, superconducting quantum interference device (SQUID) magnetometer was used to measure the particle magnetic properties and the results were compared with that of randomly oriented Ni particles of similar size obtained in previous research [8].

EXPERIMENTAL DETAILS

Ni nanoparticles and their matrix layer TiN and Al_2O_3 were deposited by ablating a pure nickel target and hot pressed TiN and Al_2O_3 target, respectively, in a pulsed laser deposition (PLD) system. Si (100) was used as the substrate. Before deposition, the silicon substrates were ultrasonically degreased and cleaned in acetone and methanol for 5 ~ 10 minutes, which was followed by 1-minute etching in 49 % hydrofluoric acid solution so that the surface silicon dioxide layer could be removed. The main deposition parameters are as follows: vacuum 5×10^{-7} Torr; substrate temperature 600° C; laser energy density 2 J/cm^2; laser frequency 10 Hz. In order to get sufficient signal during the investigation, three kinds of sample with different particle sizes (by controlling Ni deposition time) and numbers of particle layers were made: sample #1 (45 seconds and 1 layer Ni); sample #2 (30 seconds and 1 layer Ni); sample #3 (30 seconds and 5 layer of Ni separated by TiN). Particle morphology, size distribution and the crystalline quality information of both Ni particles and matrix layer were obtained through conventional and high-resolution transmission electron microscopy (TEM and HRTEM) study by JEOL 2010F and TOPCON 002B microscopes with point-point resolution of 0.18 nm. Magnetic properties of the sample were measured using superconducting quantum interference device (SQUID) magnetometer. In order to get sufficient signal, samples containing five layers of nickel separated by TiN or Al_2O_3 layer were used. Details of the measurements were published in our previous paper [8].

RESULTS AND DISCUSSION

Transmission electron microscopy study

Shown in Fig. 1 (a) is a bright filed cross-sectional image of a Ni/TiN/Si sample (#1) taken from Si [011] zone axis. As seen, uniform-sized faceted Ni nanoparticles were formed on the top of TiN matrix layer. Two distinct morphologies were found, which correspond to two different epitaxial orientation relationships and will be discussed later. Fig. 1 (b) is the corresponding selected area diffraction (SAD) pattern of Fig. 1 (a). It is easily seen that TiN was epitaxially grown on Si (100) substrate with an orientation relationship (200) TiN // (200) Si and (02 $\bar{2}$) TiN // (02 $\bar{2}$) Si. Two sets of diffraction pattern related to Ni were found: (1) cube-on-cube orientation with (200) Ni // (200) TiN and (02 $\bar{2}$) Ni // (02 $\bar{2}$) TiN; (2) (0 $\bar{2}$2) Ni // (200) TiN and (200) Ni // (02 $\bar{2}$) TiN, which is a result of 90 ° rotation with respect to the TiN [011] (zone axis). Fig. 1 (c) is a centered dark-field image formed with the circled diffraction spot in the rotated pattern of Fig.1 (b). The dark-field image study shows that the particles with a triangular morphology in [011] projection grown in the 90 ° rotated epitaxial orientation while the particles grown in cube-on-cube epitaxial relationship have a trapezoidal morphology. It was also found that some particles, like the one shown in the left side of the image, contain both orientations.

The two different epitaxial orientations corresponding to the two distinct morphologies were also found in high-resolution electron microscopy study. Fig. 2 (a) and Fig. 2 (c) are high-resolution transmission electron microscopy (HRTEM) images of nanoparticles (sample #1 and #2, respectively) taken along Si [011] zone axis. Again, the trapezoidal and triangular morphologies are clearly seen. In sample #2 the particle size is smaller than that of sample #1 due to the reduced deposition time and no particle coalescence occurred. Also shown in Fig. 2

are corresponding Fast Fourier Transform (FFT) of the two HRTEM images (Fig. 2 (b) and Fig. (d)), which confirm the above-mentioned two distinct epitaxial orientations.

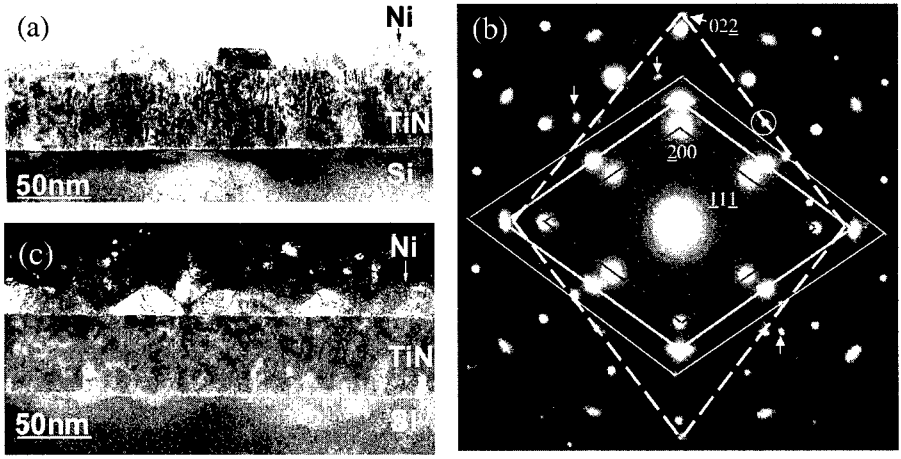

Fig.1 (a) BF image of Ni/TiN/Si sample (#1) taken from Si <011> zone axis; **(b)** The corresponding SAD pattern from the same area. Rhombus with dark, bright-wide- and bright-narrow-solid lines correspond to Si, TiN and Ni cube-on-cube epitaxial relationships, respectively. Rhombus with dashed line corresponds to 90º rotation epitaxial relationship. Note that lattice parameters calculated from the pattern corresponding to 90° rotation are slightly smaller than that of pure Ni. Arrows indicate double diffraction reflexes; **(c)** CDF image of the same area taken from the diffraction spot circled on the SAD pattern corresponding to 90º rotation (Fig.1 (b)).

Usually, in epitaxial growth, the lattice mismatch induced strain energy as well as the interfacial or chemical energy determine the orientation relationship and the epitaxial layer always orients itself in such a way that the lattice mismatch is reduced and the anisotropy interfacial energy is lowered [9]. The lattice constant of two kinds of particles could be estimated from their corresponding SAD pattern. It was found that the lattice constant of the particles grown by cube-on-cube orientation is very close to that of Ni, but the lattice constant of particles from rotated growth is apparently smaller that of pure Ni. We think that this rotated epitaxial growth was probably due to the fact that the particle formed is not pure nickel. This Ni-enriched phase was formed as a result of diffusion of foreign atoms, such as titanium. The excess titanium atoms in the TiN film would tend to diffuse to the interface and alloy during the particle growth. TiN, seen from SAD pattern and HRTEM images, is cube-on-cube epitaxially grown on Si substrate with some area of small angle misorientation. These regions could have possibly provided the diffusion path. This also could explain that in the observed area, particles with trapezoidal morphology tend to have "triangular" particles as neighbors so that particles of two morphologies are mixed. In order to explain exactly the mechanism of this rotated epitaxial

growth, future studies, such as electron energy loss spectrum (EELS) and high resolution atomic contrast imaging still need to be conducted.

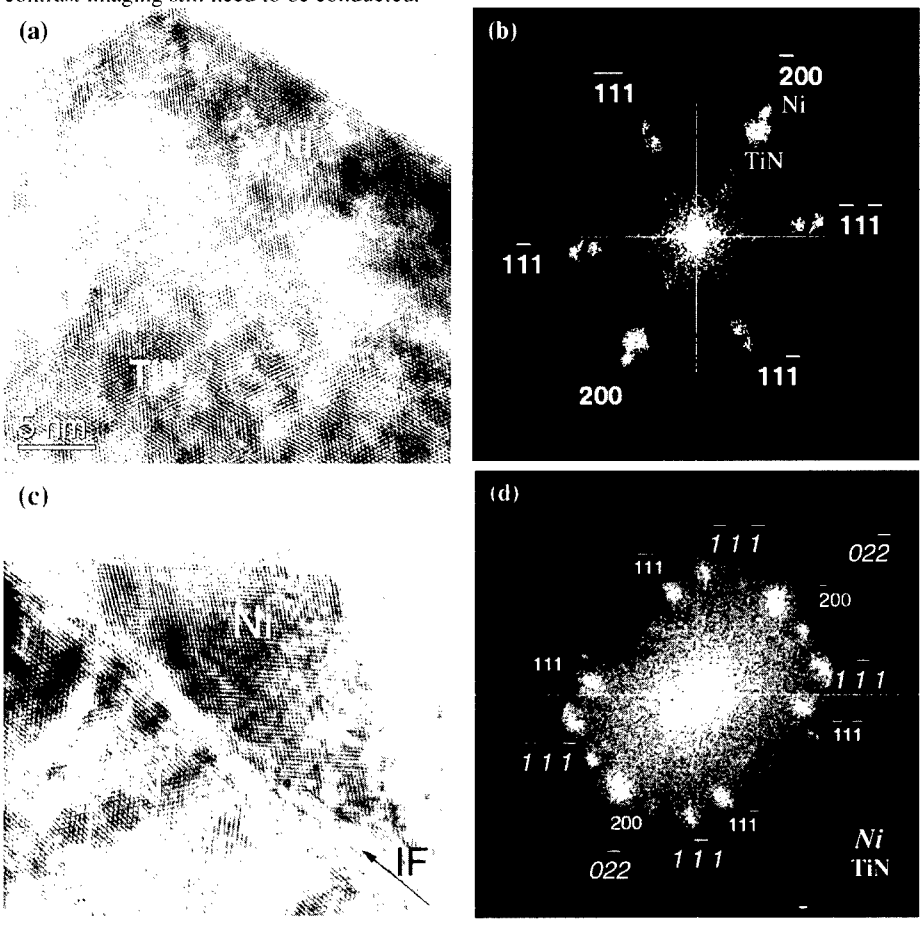

Fig.2 (a) High-resolution TEM image of a trapezoidal particle (sample #1) taken from Si <011> zone axis; **(b)** The corresponding FFT picture of (a) indicating Ni cube-on-cube epitaxial growth; **(c)** High-resolution TEM image of a triangular particle (sample #2) taken from Si <011> zone axis; **(d)** The corresponding FFT picture of (c) indicating the particle 90° rotation epitaxial growth Indexes in smaller regular numbers and bigger oblique numbers correspond to the reflections of TiN and Ni-related particle, respectively.

Magnetic measurements

Shown in Fig. 3 (a) and (b) are the ZFC and FC magnetization data as a function of temperature for Ni/Al_2O_3 sample and Ni/TiN sample (#3). The average size of Ni particles was similar in both cases. As seen, in both cases ZFC and FC curves diverge from each other at a

certain temperature, below which, ZFC curve in both cases reaches a maximum. The temperature at which this maximum occurs is known as the blocking temperature T_B. The temperature where the irreversibility sets in for two samples is quite different: 100 K for Ni/AL_2O_3 and 275 K for Ni/TiN, so is the blocking temperature. The blocking temperature for Ni on TiN matrix is around 190 K, much higher than that of Ni on Al_2O_3 matrix, which is around 30 K. Ideally, the blocking temperature and the temperature at which the irreversibility sets in ZFC and FC magnetization should be the same [6,7]. The difference in the two temperatures observed in the experiment is attributed to the size distribution of magnetic particles having different T_B [6,7].

The higher value of T_B in Ni/TiN sample with respect to that in Ni/Al_2O_3 sample is believed to be associated primarily with the texturing of Ni particles, which influences the anisotropy energy of the system. Blocking temperature is a characteristic temperature for single domain material. Below this temperature, the material shows ferromagnetic properties. As temperature increases to a certain value, the magnetic anisotropy energy, which poses the barrier for the single domain to change the magnetic orientation (magnetization vector reversal), will be overcome by thermal energy and the magnetic moments would fluctuate rapidly and freely as if a paramagnetic system, a phenomenon called superparamagnetism [10]. Above the blocking temperature the material magnetization is unstable and the sample loses any hysteric responses in the magnetization versus field measurements. The Ni particles in Ni/TiN sample grow epitaxialy via domain match on epitaxial TiN matrix [11], while the Ni particles in Ni/Al_2O_3 sample are randomly oriented due to the amorphous nature of alumina matrix. The textured nanoparticles are expected to have higher anisotropy energy. Therefore, the thermal energy required to reverse the magnetization vectors, and as a result, the blocking temperature will be higher for textured magnetic nanoparticles.

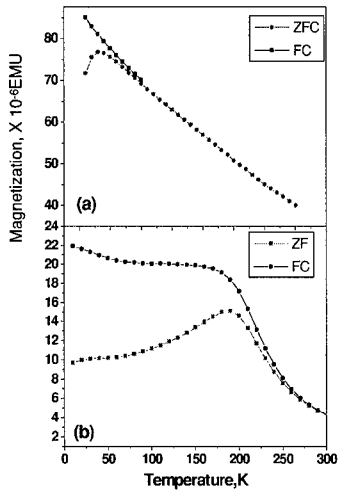

Fig. 3. ZFC and FC magnetization data as a function of temperature for (a) Ni/Al2O3 and (b) Ni/TiN samples.

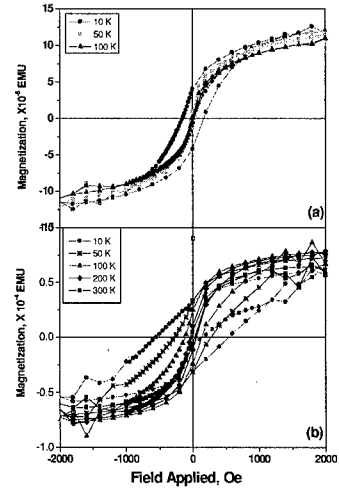

Fig. 4. Magnetization versus field curves for (a) Ni/Al_2O_3 and (b) Ni/TiN samples.

Fig. 4 shows the magnetization versus field curves for the Ni/Al_2O_3 and Ni/TiN samples. The values of H_c are found to be 25, 45, 125, 270, and 550 Oe at 300, 200, 50 and 10 K, respectively for Ni/TiN sample. The Ni/Al_2O_3 sample exhibits a coercivity ~ 150 Oe at 10 K and it is almost superparamagnetic at temperature higher than 100 K, which is in accordance with blocking temperature of Ni/Al_2O_3 sample measured form M-T plot. A comparison of the coercivity values of the two samples under several temperatures indicates that epitaxial Ni particles exhibit significantly higher coercivity than randomly oriented Ni particles. The high value of H_c of epitaxial Ni nanoparticles is envisaged to be associated with the stronger tendency of crystallographically oriented particles to retain its magnetic moments than that of randomly oriented particles under a reversing magnetic field.

CONCLUSIONS

In summary, we have fabricated textured and polycrystalline Ni nanoparticles on epitaxial TiN and amorphous Al_2O_3 matrix, respectively. The Ni particles in a Ni/TiN sample grow epitaxially because the TiN matrix layer, which grows epitaxially on Si substrate by domain match, acted as the template whereas the growth of Ni particles in Al_2O_3 matrix is polycrystalline due to the amorphous nature of alumina. Two kinds of orientation relationships related to Ni grown on TiN were found. One is cube on cube, where (200) Ni // (200) TiN // (200) Si and (02 $\bar{2}$) Ni // (02 $\bar{2}$) TiN // (02 $\bar{2}$) Si and the particles grown in this orientation have a trapezoidal morphology in the [011] projection. The other involves a 90 ° degree rotation with respect to [011] direction of TiN matrix, where (0 $\bar{2}$2) Ni // (200) TiN // (200) Si and (200) Ni // (02 $\bar{2}$) TiN // (02 $\bar{2}$) Si. The particles grown in this orientation have a triangular morphology in the [011] projection and a smaller lattice constant compared to that of pure nickel. The blocking temperature of the Ni/TiN sample (~190 K) is significantly higher than that of Ni/Al_2O_3 sample (~30 K) with similar size of embedded magnetic particles. A comparison of the values of coercivity (H_c) of the two samples has shown that epitaxial Ni particles also exhibit significantly higher coercivity than polycrystalline randomly oriented Ni particles.

ACKNOWLEDGMENTS

This research was supported by the US National Science Foundation Center for Advanced Materials and Smart Structures.

REFERENCES

1. A.P. Alivisatos, Science **271,** 933 (1996).
2. C. B. Murry, C. R. Kagan and M. G. Bawendi, Science **270**, 1335 (1995).
3. V. F. Puntes, K. M. Krishnan and A.P. Alivisatos, Appl. Phys. Lett. **78**, 2187 (2001).
4. J. L. Dorman, D. Fiorani and E. Tronc, Adv. Chem. Phys. **98**, 283 (1997).
5. A. S. Edelstein and R. C. Cammarata, *Nanomaterials: Synthesis, Properties and Applications* (IOP, Bristol, 1998).
6. W. Luo, S. R. Nagel, T. F.Rosenbaum, and R. E. Rosensweig, Phys. Rev. Lett. **67**, 2721 (1991).
7. R. W. Chantrell, N. S. Walmsey, J. Gore and M. Maylin, Appl. Phys. Lett. **85**, 4320 (1999).
8. D. Kumar, H. Zhou, T. K. Nath, A. Kvit and J. Narayan, Appl. Phys. Lett. **79**, 2817 (2001).

9. T. Zheleva, K. Jagannadham and J. Narayan, J. Appl. Phys.**75**, 860 (1994).
10. C. L. Chien, Nanostructured Materials **1**, 179 (1992).
11. J. Narayan, US Patent No. 5,406,123 (11 April, 1995).